An "Inverse Conglomerate" Paleomagnetic Test and Timing of In Situ Terra Rossa Formation at Bloomington, Indiana

Joseph G. Meert, Frank D. Pruett,[1] *and Enrique Merino*[2]

Department of Geological Sciences, 241 Williamson Hall, Gainesville, Florida 32611, U.S.A.
(e-mail: jmeert@ufl.edu)

ABSTRACT

Directions of remanent magnetism in an ~2-m interval of terra rossa claystone at Bloomington, Indiana, cluster around the current Earth magnetic field direction, a fact consistent with authigenic formation of the terra rossa over the last 0.78 m.yr., the date of the latest earth's magnetic field reversal, and suggesting a minimum terra rossa formation rate of ~2.5 m/m.yr. Paleomagnetic directions in limestone "floaters" within the terra rossa are indistinguishable from directions of the bedrock Mississippian Harrodsburg Limestone, indicating that the floaters are in situ and perfectly preserve their original stratigraphic position. Thus, the red claystone containing the floaters is interpreted as an authigenic, isovolumetric replacement of the Harrodsburg—the replacement of which the floaters escaped—and precludes the possibility that the floaters and the surrounding claystone are a mudflow that had carried limestone blocks in it. The implication that the claystone is authigenic independently confirms the petrographic observations reported previously that the red clay grew in situ, replacing the underlying limestone at a moving metasomatic front. Rock magnetic studies of the terra rossa clays show evidence of both goethite and maghemite as main magnetic carriers of this remanence. Both minerals are independently known to occur in pisolites of the terra rossa. The ferric-iron-bearing red clays also are weakly magnetic.

Introduction

Terra rossa clays are claystones up to several meters thick and kilometers across that occur at the earth's surface and are associated with karst carbonates. There are terra rossas across southern Europe; south Australia; southern China; the Caribbean; Texas, Indiana, Kentucky, and Florida in the United States; and elsewhere. This article is the third in a series devoted to the genesis of terra rossa clays. In the first article, Merino and Banerjee (2008) presented field and petrographic evidence that the terra rossa occurring on the Mississippian limestones at Bloomington, Indiana, was formed by replacement of limestone by authigenic clays and minor iron oxides at a thin reaction front at the base of the existing terra rossa. In their model, the major elements required to make the authigenic clays—Fe, Al, Si—come from dust dissolved at the surface. The dissolved species infiltrate down to the current replacement front, where they combine to make new clay minerals. As the clay-for-calcite replacement front deepens, it leaves behind a massive terra rossa within which there may occur limestone blocks of a range of sizes; in Bloomington, these are referred to as "floaters" that escaped replacement and are completely surrounded by red clay (fig. 1). This is inherently an isovolumetric process (Nahon and Merino 1997), and if the terra rossa formed by replacement of the limestone, then the remnant limestone floaters within it should be in their proper stratigraphic orientations within the profile. Significantly, in a rock magnetic study, Mathé et al. (1999) showed that the saprolite portion of weathering profiles on silicate parent rocks in Cameroon and Morocco also preserves bulk volume, confirming the petrographic and field evidence that they form basically through replacement (Merino et al. 1993). The reason replacement automatically preserves bulk volume was explained by Nahon and Merino (1997, p. 408,

Manuscript received July 16, 2008; accepted November 7, 2008.

[1] Indiana Geosciences Institute, 2000 Olcott Boulevard, Bloomington, Indiana 47401, U.S.A.; e-mail: sfpruett@sbcglobal.net.

[2] Department of Geological Sciences, Indiana University, Bloomington, Indiana 47405, U.S.A.; e-mail: merino@indiana.edu.

[The Journal of Geology, 2009, volume 117, p. 126–138] 0022-1376/2009/11702-0002$15.00 DOI: 10.1086/596108

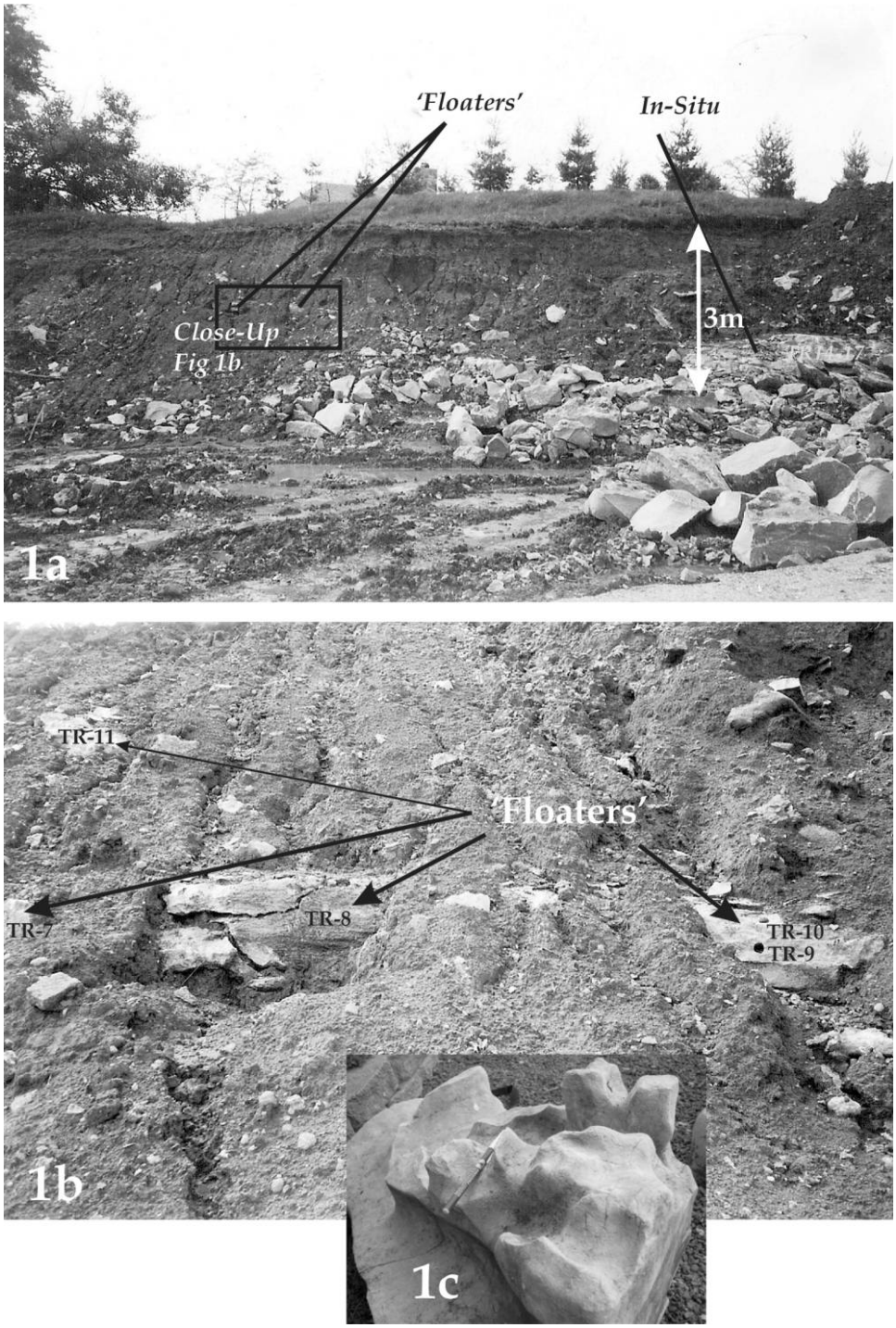

Figure 1. *a*, Wide view of the terra rossa outcrop at Tenth Street and Smith Road in Bloomington, Indiana. About 3 m of terra rossa clays are underlain by bedrock Mississippian Harrodsburg limestone that outcrops only at lower right. Not all sample locations are visible in this photo. *b*, Close-up of limestone "floaters" within the terra rossa clays. *c*, Floater (not from the outcrop in *a*) exhibiting typical concave shapes and wormholes produced by the reactive infiltration instability, triggered by the replacement of limestone by clay (Merino and Banerjee 2008).

their fig. 7), who present a detailed analysis of solid volume replacement (see also Merino and Banerjee 2008).

A. Banerjee and E. Merino (unpublished manuscript) propose a reaction-transport model based on the chemical dynamics proposed by Merino and

Banerjee (2008). The model predicts values of the velocity of the terra-rossa-producing front that reasonably match our estimates, which are based on the paleomagnetic data presented here.

The purpose of this investigation is to determine by paleomagnetic methods whether the floaters in figure 1*a*, 1*b* are in their original stratigraphic positions. A second purpose is to constrain the timing of terra rossa formation in the region of Bloomington, Indiana (fig. 2). This independent determination constitutes an additional test for the predicted rate of terra rossa formation predicted by quantitative modeling by A. Banerjee and E. Merino (unpublished manuscript). This study is based on measurements of remanent magnetization intensities and directions of the terra rossa, along with those of the

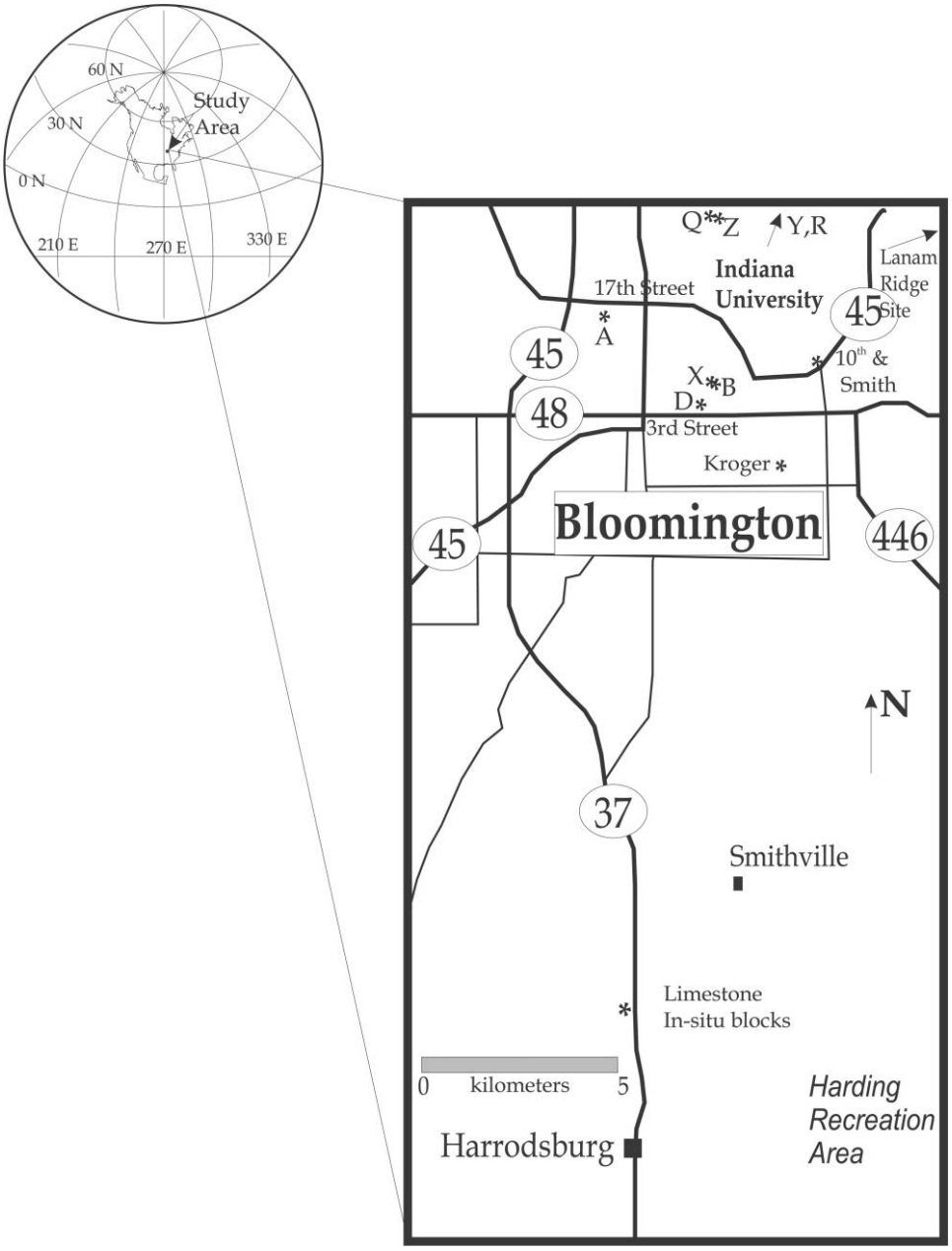

Figure 2. Map of sampling sites in this study. Letter sites (*A*, *B*, etc.) are from the study by Pruett (1959). Outcrops collected in 1998 and 2002 are designated by site names (Harrodsburg, Tenth and Smith, etc.). The Lanam Ridge site is approximately due east of the site at Tenth Street and Smith Road. Sites Y and R (terra rossa soils) are located several miles to the north of the map.

limestone floaters and of in situ bedrock limestones in the region.

The terra rossa at Bloomington, Indiana, consists of 7-, 10-, and expandable 13-Å clays and minor iron oxide pisolites, plus minor admixed quartz and feldspar eolian silt. The 7-Å clay is Fe^{3+}-bearing kaolinite that was identified optically. The 10-Å and 13-Å clays are probably illite and smectite also containing Fe^{3+} (and other cations), but neither has been identified optically. The pisolites in many terra rossa thin sections are very dark brown to black, up to 2 mm in size, and composed of iron oxides. Eroded pisolites up to 1 cm in size can be found near terra rossa outcrops. Some pisolites are strongly magnetic, probably consisting of maghemite (Pruett 1959), but most others consist of goethite (detected by x-ray diffraction). The pisolites are authigenic, not inherited from the underlying Salem or Harrodsburg Limestones, which are Mississippian calcarenites consisting of well-cemented bryozoan and echinoderm fragments. By chemical analysis, they contain about 0.2–0.3 wt% Fe_2O_3 and 0.05 wt% MnO (analyses provided by the Indiana Geological Survey).

Sampling and Methods

The three sets of samples that were studied were collected in spring 1998 and summer 2002. The outcrops of terra rossa in Bloomington are opportunistic targets because good profiles are available only when construction crews excavate an area for building purposes. Most of these outcrops are covered up on completion of the construction. One set of samples of terra rossa, limestone floaters, and bedrock limestone was taken from an outcrop opened by the city of Bloomington, Indiana, to smooth the intersection of Tenth Street and Smith Road. The outcrop was 11 m long and about 3 m high (fig. 1*a*, 1*b*). Sample locations are shown in figure 1*a*, 1*b*. Twelve additional samples of terra rossa covering a total thickness of 1.8 m were obtained from a second outcrop, Lanam Ridge. A second set of bedrock Harrodsburg limestone samples was collected from Highway 37 just south of Bloomington.

Paleomagnetic samples of limestone were drilled in the field with a gasoline-powered hand drill and oriented using both sun and magnetic compass. Limestone samples were then cut into standard-

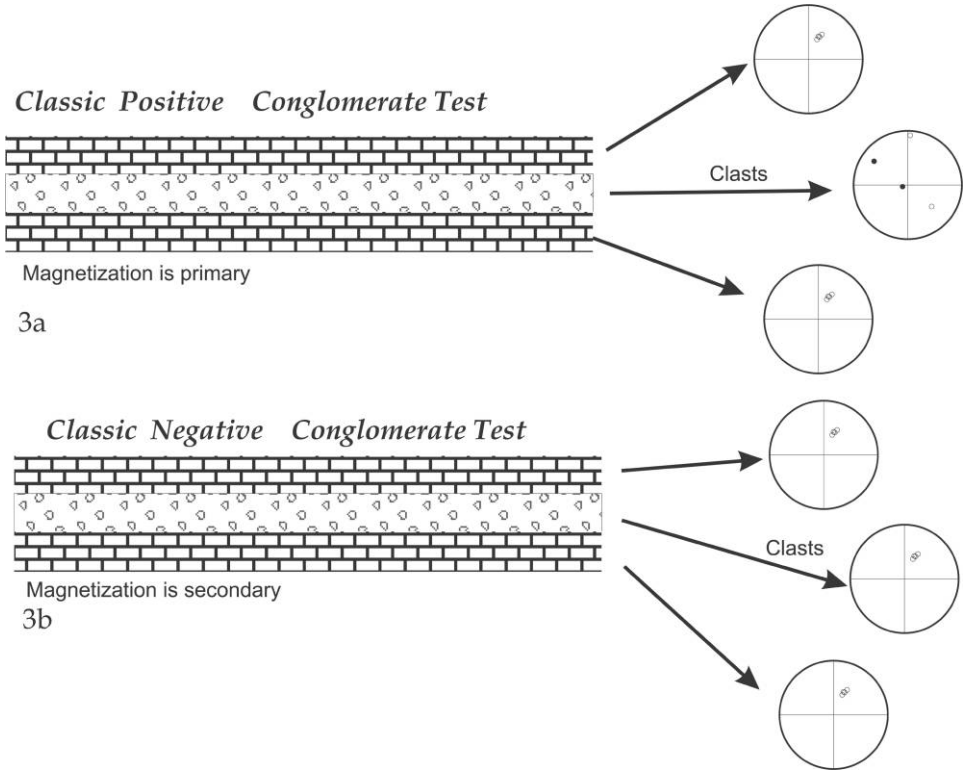

Figure 3. The intraformational conglomerate test in paleomagnetism. *a*, Positive: samples from the units above and below the conglomerate show consistent directions, whereas the clasts of similar material from the conglomerate show random directions. *b*, Negative: samples from the clasts and units above and below all show the same direction.

sized paleomagnetic specimens (12.54 cm^3 cylinders) for analysis on a Superconducting Technologies cryogenic magnetometer at the University of Florida. Limestone samples were stepwise demagnetized using either alternating field or thermal methods.

Samples of the terra rossa clays were collected in 8-cm^3 plastic boxes by pushing the boxes horizontally into the clay, removing the sample and then orienting the vacated hole using a magnetic compass. The magnetization direction of the terra rossa clay samples was measured, and then the samples were treated with a blanket alternating field of 130 mT.

The "Inverse Conglomerate Test"

The classic conglomerate test in paleomagnetic studies relies on the fact that boulders within a conglomeratic sequence can either retain a stable ancient remanence or be completely remagnetized following deposition of the boulders. We will discuss ideal cases here for illustrative purposes.

A traditional conglomerate test relies on an intraformational conglomerate wherein stable magnetization directions are found in nonconglomeratic units above and below the conglomerate (fig. 3*a*). If the directions in the conglomeratic clasts show a demagnetization behavior similar to their parent materials but yield a random directional grouping (due to their "tumbling" during deposition), then the magnetization in the underlying units is unlikely to have been reset. On the other hand, if the clasts, the overlying unit, and the underlying unit all show similar directions, then it is probable that the remagnetization postdates the formation of the conglomerate (fig. 3*b*).

In this article, we use a modification of the conglomerate test to check paleomagnetically whether the limestone floaters in the terra rossa clays occur in their original in situ orientations and, therefore, whether the surrounding terra rossa clay

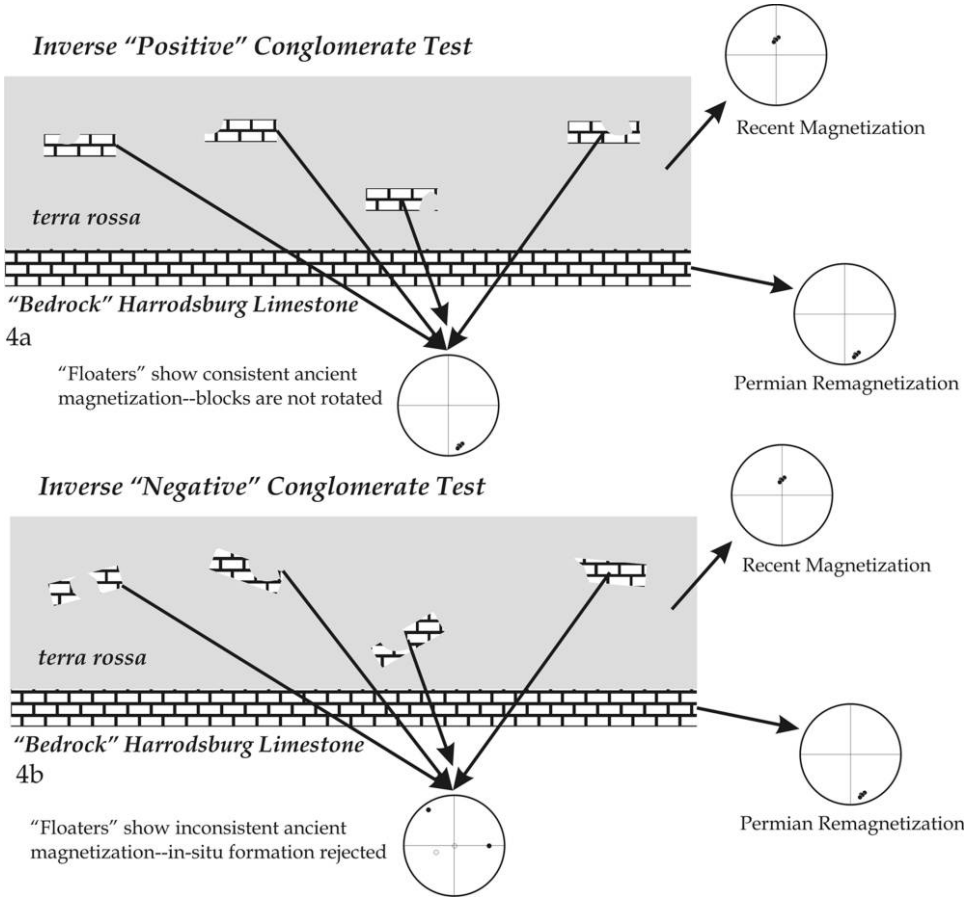

Figure 4. *a*, Inverse positive conglomerate test: both "floaters" and in situ limestones show the same directions, whereas the surrounding terra rossa claystone shows more recent paleomagnetic directions. *b*, Inverse negative conglomerate test: floaters, terra rossa claystone, and in situ limestones all show different directions.

grew in situ, isovolumetrically replacing the limestone rather than accumulating as detrital clay. The formation of terra rossa is a relatively recent event (see next section) and the Harrodsburg limestone in the region is of Mississippian age. Therefore, all things being equal, the bedrock and the claystone should show distinct paleomagnetic directions. The recent time-averaged (<780-ka) magnetic field direction at Bloomington, Indiana (latitude 39°N), should be due north with an inclination of $\sim +58°$. Paleozoic limestones in the central United States show a ubiquitous late Paleozoic (~Permian age) remagnetization (McElhinny and McFadden 2000) that is directed to the southeast and has a shallow inclination.

If the magnetization in the limestone floaters is similar in direction to in situ bedrock limestone in the Bloomington region, then a solid argument can be made that the limestone blocks now surrounded by terra rossa clays remained in their original positions during formation of the terra rossa clays. Therefore, the terra rossa that surrounds the floaters would have formed by replacement of the original bedrock of which the floater is the unreplaced in situ part (fig. 4*a*). If the floaters within the terra rossa had been either rotated or transported, then the magnetization directions in those blocks should yield randomly directed magnetizations. If the directions are random, then this observation would negate arguments favoring in situ replacement models for the formation of terra rossa clays (fig. 4*b*).

Paleomagnetic Results

Terra Rossa Clays. Three suites of terra rossa samples were analyzed following the 1998 field session. Terra rossa samples collected in cubes showed fairly good clustering about the current Earth field direction before alternating field demagnetization. Directions showed better clustering after being subjected to a blanket demagnetizing field of 130 mT. The mean paleomagnetic direction for the three sites collected in the 1998 field season was declination = 352.2°, inclination = +58.4° ($k = 119$, $\alpha_{95} = 11°$, $n = 3$ sites), with a pole located at 84°N, 185°E (table 1). The pole overlaps with the time-averaged dipole field pole located at 90°N, 0°E (see figs. 5, 6).

Nine sites in terra rossa were also collected by Pruett (1959); although those samples were not subjected to any demagnetization, they were used to augment our analysis (table 1). One site (site C) in that study had only three samples, and a second site (site A) yielded a poorly clustered mean with a large α_{95} value (32°). These two sites were not used in compiling the mean reported in table 1. Although the other sites had relatively low k values (precision parameter; Fisher 1953) ranging from 8 to 29, the overall means from those sites are similar to the mean obtained from our 1998 samples and the site means show excellent clustering ($k = 97$). The overall mean direction from the six sites of Pruett (1959) is declination = 6.5° and inclination = +58.6° ($k = 97$, $\alpha_{95} = 6.8°$) with a pole position located at 85°N, 359°E (see figs. 5, 6).

Table 1. Paleomagnetic Results

Si	n/N	Dec.	Inc.	k	α_{95}	P.lat.	P.long.
TR clays at Smith Road and Tenth Street	6/10	348°	62.8°	44	10.2°	80°N	217°E
TR clays at Lanam Ridgeview Estates	10/11	004°	54.1°	56	6.5°	85°N	056°E
TR clays at Kroger	12/12	343°	57.4°	82	4.8°	77°N	184°E
Mean TR clays	3 sites	352.2°	58.4°	119	11°	84°N	185°E
TR site A (Pruett 1959)[a]	6/10	32°	56°	5.2	32°	65°N	359°E
TR site B (Pruett 1959)	15/15	20.4°	68°	29	7.2°	72°N	317°E
TR site D (Pruett 1959)	9/9	15°	63.4°	16	13.4°	78°N	331°E
TR site Q (Pruett 1959)	48/60	2°	59.1°	10	7.1°	88°N	340°E
TR site R (Pruett 1959)	5/6	11.4°	53.6°	13	22.1°	80°N	029°E
TR site Y (Pruett 1959)	43/44	1.4°	49.1°	16	5.5°	81°N	086°E
TR site Z (Pruett 1959)	53/56	355°	57°	8	7.4°	86°N	163°E
Mean TR (Pruett)	6/7 sites	6.5°	58.6°	97	6.8°	85°N	359°E
Combined mean, TR clays	9/10 sites	2°	58.7°	94	5.3°	88°N	352°E
Limestone at Highway 37	12/18	171.8°	+14°	29	8.3°	43°N	106°E
Harrodsburg limestone blocks beneath TR clays	7/7	161°	+10°	79	7°	44°N	120°E
Limestone "floaters"	6/7	157°	+28°	18	16°	33°N	120°E
Mean results, limestone	3 results	163.4°	+17.4°	46	18°	39.7°N	115°E

Note. TR = terra rossa, n/N = samples used/samples collected, Dec. = declination, Inc. = inclination, k = precision parameter, α_{95} = circle of95%confidence about the mean direction, P.lat. = latitude of the paleomagnetic pole or virtual geomagnetic pole, P.long. = longitude of the paleomagnetic pole or virtual geomagnetic pole.

[a] Not used in the mean results. Reduced to common site latitude and longitude 39.165°N, 86.53°W.

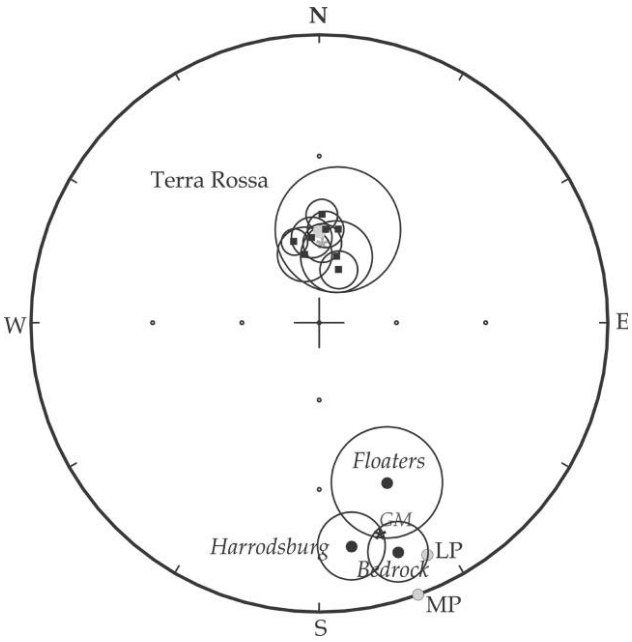

Figure 5. Stereographic projection of terra rossa mean directions (*squares*) along with results from the limestone samples from the sites in this study (*circles*). The overall mean direction from all terra rossa sites is shown as a light gray circle, and the dipole field direction for the current Earth magnetic field is shown as a gray cross. Harrodsburg limestones in situ; *Bedrock* = limestones at the base of the outcrop at Tenth Street and Smith Road in situ and limestone "floaters" at the outcrop of Tenth Street and Smith Road; *GM* (*star*) = grand mean of limestone samples, *MP* = Middle Permian predicted direction from North American apparent polar wander path (APWP), and *LP* = Late Permian predicted direction from North American APWP (McElhinny and McFadden 2000).

We calculated an overall mean direction for the terra rossa samples by combining the 1998 results with the results from Pruett (1959). The overall mean direction from nine sites has a declination = 2° and an inclination = +58.7° ($k = 94$, $\alpha_{95} = 5.3°$) and a resultant paleomagnetic pole calculated at 88°N, 352°E. The overall mean pole is indistinguishable from the time-averaged dipole field average at 90°N, 0°E (table 1; figs. 5, 6).

Limestones. Samples from in situ bedrock limestones near Harrodsburg, Indiana (fig. 2), and beneath the terra rossa clays at Tenth Street and Smith Road (fig. 2) were stepwise demagnetized using either thermal or alternating field methods. Thermal demagnetization yielded more clearly defined directions. All samples with clearly defined trajectories showed a trend toward the southeast and shallowly positive inclinations (figs. 6, 7*a*). Magnetization directions in the limestone samples became noisy above ~300°C, and so directions were chosen on the basis of linear segments when available (fig. 7) or intersections of great-circle trajectories. Table 1 lists the results for the limestones from Highway 37. Twelve of a total of 18 samples yielded a site mean direction of declination = 171.8° and inclination = +14° ($k = 29$, $\alpha_{95} = 8.3°$; fig. 5). A virtual geomagnetic pole (VGP) from these limestones falls at 43°N and 106°E (fig. 6). All seven limestone samples from Tenth and Smith yielded consistent results (fig. 7*b*). The mean direction of the in situ limestones at Tenth Street and Smith Road is declination = 161° and inclination = +10° ($k = 79$, $\alpha_{95} = 7°$). A virtual geomagnetic pole from these samples falls at 44°N, 120°E (fig. 6).

Samples from limestone floaters within the terra rossa at Tenth Street and Smith Road were subjected to stepwise thermal demagnetization. These samples exhibited behavior similar to that observed in the in situ limestone samples (fig. 7*c*). Table 1 lists the results from these floaters. Six of a total of seven samples yield consistent data with a mean declination = 157° and an inclination = +28° ($k = 18$, $\alpha_{95} = 16°$; table 1; fig. 5). A virtual geomagnetic pole from these samples falls at 33°N, 120°E (fig. 6). Some of the samples (fig. 7*c*) show an overprint at very low temperature steps that is identical to that observed in the terra rossa, but the higher temperature magnetizations that we believe are carried by magnetite are consistent with the Permian directions seen in other limestone samples in the area. The VGPs and magnetization directions from the in situ limestones are statistically indistinguishable from the floaters and all are statistically different from directions in the terra rossa clay samples (fig. 5).

Rock Magnetism

Rock magnetic tests (for a complete discussion, see McElhinny and McFadden 2000) attempt to characterize the magnetic carriers in rocks by examining their (1) magnetic intensity changes during increasing magnetic fields at room temperature (isothermal remanence acquisition = IRM) and their (2) magnetic susceptibility changes during stepwise heating (Curie temperature runs).

To further characterize the magnetic carriers in the limestone samples and the terra rossa clays, we conducted IRM studies. None of the limestone samples reach full saturation in a maximum field of 1.3 T. Samples from in situ limestones collected along Highway 37 reached 75%–85% of their maxi-

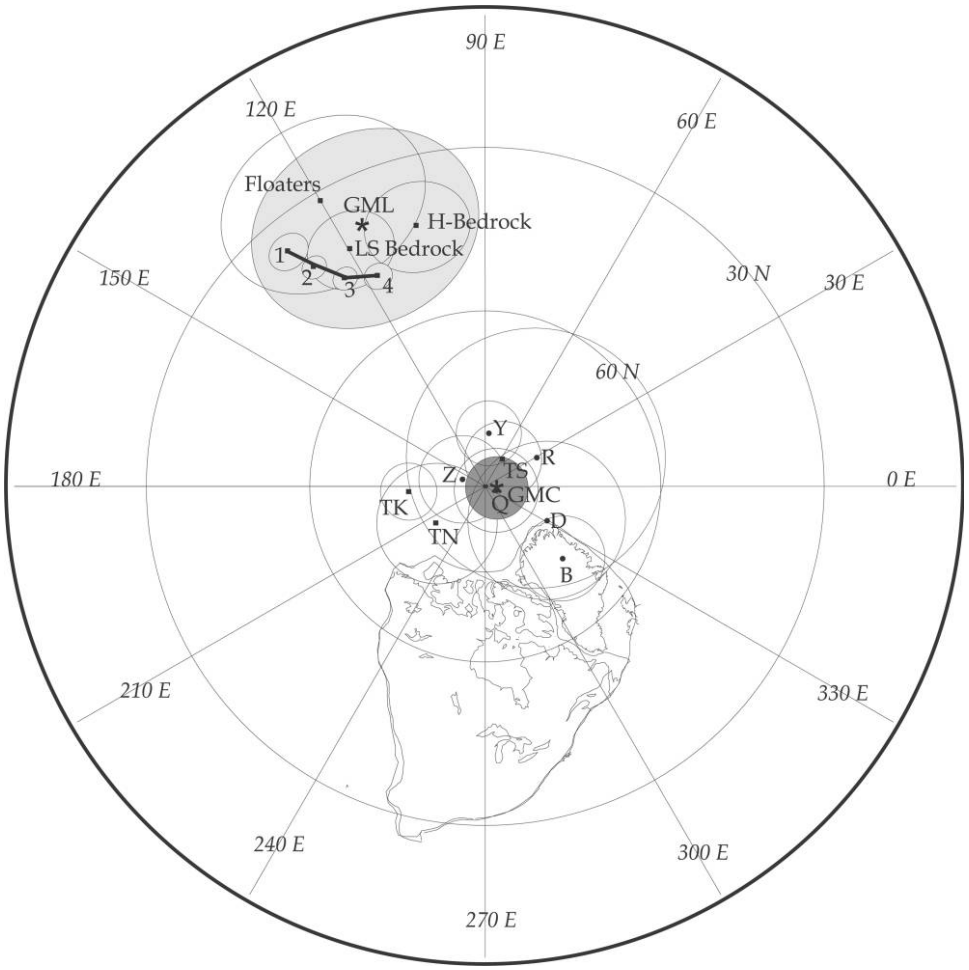

Figure 6. Virtual geomagnetic poles calculated from the sites listed in table 1. Sites from the terra rossa clay samples: squares are from demagnetized terra rossa clays (*TK* = Kroger samples, *TN* = Smith Road and Tenth Street, and *TS* = Lanam Ridge site); circles are from the study by Pruett (1959) and are keyed to the lettered sites in table 1. *GMC* = grand mean pole from table 1 for terra rossa clays is designated by the star inside the dark gray α_{95} circle. Blue α_{95} circles are mean directions calculated from in situ limestones along Highway 37 (*H-bedrock*), in situ limestone blocks at Tenth Street and Smith Road (*LS bedrock*), and limestone "floaters" collected at Tenth Street and Smith Road (*Floaters*). The grand mean calculated from all limestone sites is designated in light gray α_{95} as *GML*. The numbered circles show the apparent polar wander path for Laurentia from Late Carboniferous (*1*) to early Permian (*2*) to mid-Permian (*3*) to Late Permian-Triassic (*4*).

mum intensity by 0.3 T, suggesting a major contribution from magnetite (fig. 8*a*). The slow rise after 0.3 T is attributed to alteration to higher coercivity hematite or goethite (Heller 1978). In contrast, limestone floaters reached only about 50% of their maximum intensity by 0.3 T, and both samples showed a steady increase in intensity with applied field (fig. 8*a*). This is consistent with a magnetization dominated by hematite or goethite (Heller 1978). One sample of in situ limestone beneath the terra rossa clays reaches ~65% of maximum intensity by 0.3 T followed by a slow rise at higher applied fields, suggestive of mixing between a magnetite/maghemite and hematite/goethite signal (fig. 8*a*; Heller 1978).

Samples from terra rossa clays at Lanam Ridge also show a range in behavior on application of IRM fields of 1.2 T (fig. 8*b*). Two samples (LAN-3 and LAN-4) reach more than 90% of their maximum intensity by 0.1 T. Such a signal is typical of low-coercivity phases like magnetite or maghemite. In contrast, samples LAN-1 and LAN-2 show much slower increases in intensity with applied field. This behavior is more typical of a hematite/goethite-dominated mineralogy with minor contributions from either magnetite or maghemite. Maxi-

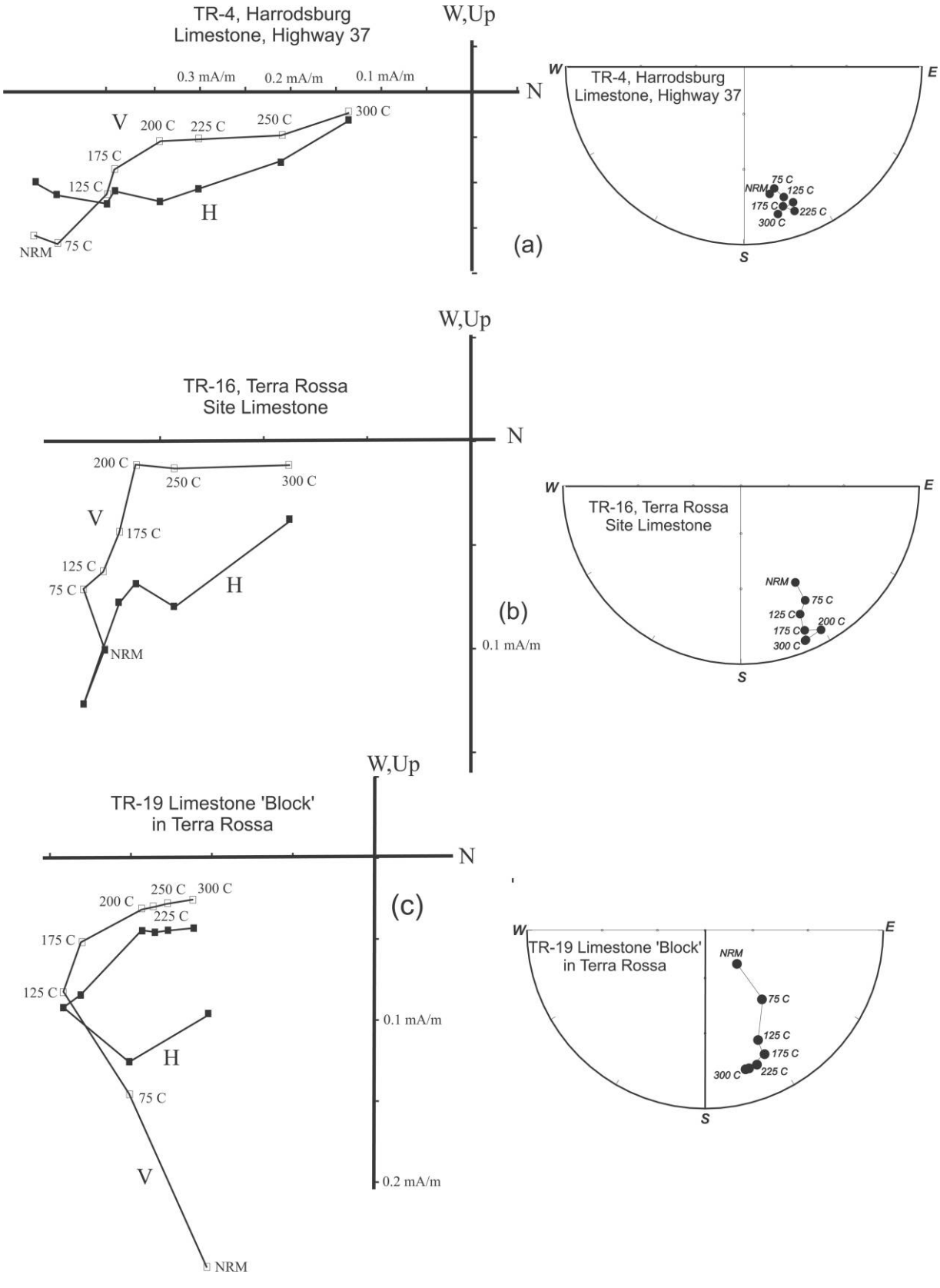
TR-4, Harrodsburg
Limestone, Highway 37
W,Up
0.3 mA/m
0.2 mA/m
0.1 mA/m
N
V
200 C
225 C
250 C
300 C
175 C
125 C
H
NRM
75 C
(a)
W
E
S
TR-4, Harrodsburg
Limestone, Highway 37
NRM
75 C
125 C
175 C
225 C
300 C
W,Up
TR-16, Terra Rossa
Site Limestone
N
200 C
250 C
300 C
V
175 C
125 C
75 C
H
NRM
(b)
0.1 mA/m
W
E
S
TR-16, Terra Rossa
Site Limestone
NRM
75 C
125 C
175 C
200 C
300 C
W,Up
TR-19 Limestone 'Block'
in Terra Rossa
N
250 C
300 C
200 C
225 C
175 C
125 C
H
75 C
V
NRM
(c)
0.1 mA/m
0.2 mA/m
W
E
S
TR-19 Limestone 'Block'
in Terra Rossa
NRM
75 C
125 C
175 C
300 C
225 C

mum IRM intensities in samples LAN-3 and LAN-4 are on the order of $3–5 \times 10^3$ mA/m^2, sample LAN-2 has an intensity of 2×10^2 mA/m^2, and sample LAN-1 has an intensity of 4×10^1 mA/m^2. The intensities observed in the IRM studies are consistent with the magnetite/maghemite mineralogies (LAN-3 and LAN-4), hematite/goethite mineralogy (LAN-1), and a combination of both (LAN-2).

Curie temperature analyses on four terra rossa clay samples from Lanam Ridge (samples LAN-1–4) and two hand samples of terra rossa show evidence of alteration during heating, probably due to the presence of organic carbon and water (fig. 9*a*–9*d*; see also Hanesch et al. 2006). Sample LAN-3 shows a slight increase in susceptibility beginning around 275°C and a monotonic drop in susceptibility beginning at 400°C (fig. 9*a*). An estimated Curie temperature based on the heating phase is ~575°C, and a conversion to hematite is demonstrated by the slight increase in susceptibility above 575°C, consistent with maghemite-goethite converting to hematite (fig. 9*a*). Sample LAN-4 shows a nearly reversible Curie temperature curve with a $T_C \sim 535$°C. A slight inflection beginning around 400°C may reflect partial alteration of some of the maghemite to hematite. The cooling curve is dominated by a ferromagnetic mineral, probably either maghemite or magnetite (fig. 9*b*). Sample HS0 shows a decrease in susceptibility between about 350° and 480°C. On cooling, the sample shows a small Hopkinson peak and an increase in susceptibility (fig. 9*c*). We speculate that this behavior (during laboratory heating) could result from a possible reduction of maghemite to magnetite in a reducing environment facilitated by organic carbon in the terra rossa (see also Hanesch et al. 2006). Sample HS-1 shows a large increase in susceptibility at ~460°C and a rapid decrease in susceptibility at ~575°C (fig. 9*d*). Again here, we speculate that this intensity increase results from the reduction of maghemite to magnetite. On cooling, a very large increase in susceptibility is observed (note the difference in cooling scale vs. heating K scale). Hanesch et al. (2006) noted that the presence of organic carbon can result in reducing conditions during heating; the large change in susceptibility during cooling is probably the conversion of maghemite to magnetite. The Hopkinson peak (characteristic of pure magnetite) is evident in the cooling curve, and the Curie temp falls at 575°C (fig. 9*d*). Finally, a small sample of the clay-size-only fraction of material from the terra rossa soils was separated for a Curie temperature run. Although the susceptibility of this fraction is much lower, it is apparent that the clay-size fraction shows a steady decline in susceptibility (fig. 9*e*) beginning at ~450°C and a nearly reversible susceptibility curve on cooling (suggesting that this fraction is not altered during heating).

Discussion

Magnetization directions from the terra rossa at Bloomington show some scatter in direction (declination = 2°, inclination = +58.7°; fig. 5), and an overall cluster around the time-averaged present-day field direction (declination: 0°, inclination = +58.4°). The results include data collected in the late 1950s that were not subjected to demagnetization. In spite of this, the overall mean direction from those sites is also of a single polarity clustering around the time-averaged present-day field direction. We interpret these data to indicate that the youngest few meters of terra rossa clays at Bloomington have formed during the present Bruhnes normal polarity chron; thus, the terra rossa is <0.78 m.yr. old (Opdyke and Channell 1996). Our conclusion is similar to the findings on terra rossa from the Yun-Gui Plateau in southwest China of Feng et al. (2003), who also found a Bruhnes-age magnetization. Our paleomagnetically determined age estimate provides a minimum rate of terra rossa formation of 2.5m/m.yr. (2 m/0.78 m.yr.) and allows an independent check of the reaction-transport rates of 1–3 m/m.yr. estimated by A. Banerjee and E. Merino (unpublished manuscript).

Limestone samples from the Harrodsburg Formation along Highway 37 and samples collected from the base of the terra rossa section at Tenth Street and Smith Rd (fig. 2) show variable demag-

Figure 7. *a*, Orthogonal vector diagram and stereographic projection of the stepwise demagnetization of sample TR-4 (Harrodsburg limestone; Highway 37, south of Bloomington, IN). Samples here show a nearly univectorial decay to the origin. *b*, Orthogonal vector diagram stereographic projection of stepwise demagnetization behavior of sample TR-16, an in situ limestone beneath the terra rossa clays at Tenth Street and Smith Road. *c*, Orthogonal vector diagram stereographic projection of stepwise demagnetization behavior of sample TR-19, a limestone "floater" from Tenth Street and Smith Road. Samples progress along a great-circle trajectory toward a southeast, shallow down direction characteristic of a Late Paleozoic remagnetization (see text for details).

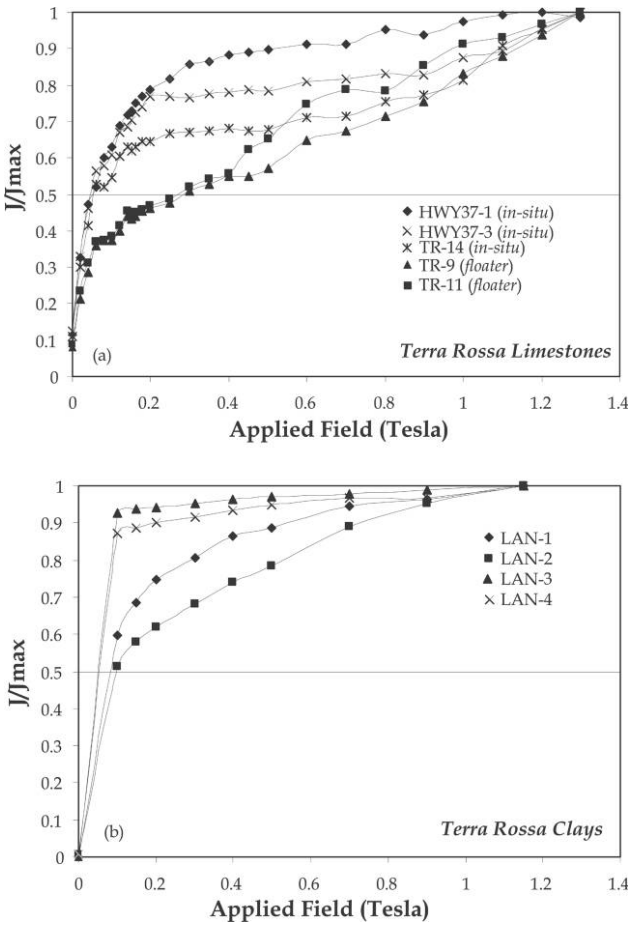

Figure 8. *a*, Isothermal remanence acquisition studies from limestone samples in this study. *b*, Isothermal remanence acquisition studies from terra rossa soils in this study. See text for details.

netization behavior. A few samples show only a northerly and intermediate positive inclination, consistent with a recent overprint. Most show a more complex behavior with demagnetization, the vectors moving along a great-circle trajectory toward a southeast-directed and shallow positive inclination (fig. 7). A comparison of these directions to the well-defined late Paleozoic North American apparent polar wander path (APWP) indicates coincidence with the Permian segment of the APWP (fig. 6). A pervasive secondary magnetization of Permian age is well known in Paleozoic limestones of the North American midcontinent, and we attribute these directions to the Permian field (McElhinny and McFadden 2000).

The limestone samples from floaters within the terra rossa show demagnetization behavior identical to that of in situ limestones and yield a southeast and shallow positive direction (fig. 7*c*; table 1). Thus, the observed directions of magnetization in the limestone floaters provide evidence of a positive inverse conglomerate test (fig. 7*c*). The consistency between in situ limestone samples and floater samples supports our contention that the limestone floaters have not changed their orientations during terra rossa formation, and this confirms the in situ replacement origin detected petrographically by Merino and Banerjee (2008).

Conclusions

A paleomagnetic investigation of terra rossa clays and limestones near Bloomington, Indiana, yields data that are consistent with the hypothesis that the 2–3 m of terra rossa formed via in situ replacement of the Mississippian Harrodsburg limestone during the Bruhnes Epoch (<0.78 Ma). This yields a minimum growth rate of the terra rossa of 2.5 m/m.yr., a number against which A. Banerjee and E. Merino (unpublished manuscript) compare their reaction-transport predictions of the rate of terra rossa formation. Rock magnetic studies (IRM and Curie temperature) of the terra rossa clays show evidence that goethite and maghemite are the main magnetic carriers of this remanence. Both minerals are independently known to occur in pisolites of the terra rossa.

Significant volumetric increases or decreases of bulk volume during formation of the terra rossa by replacement would could cause rotation or slumping of the limestone floaters and would result in a mechanical dispersion of their originally acquired magnetization directions. Thus, the absence of physical disruption in the limestone floaters as evidenced by the inverse conglomerate test supports an isovolumetric (or nearly so) replacement of limestone by terra rossa. Mathé et al. (1999) also inferred from magnetic susceptibility studies (AMS) of laterites in Morocco and Cameroon that saprolitization was constant volume. Further evidence for in situ formation of terra rossa is provided by the AMS studies of Feng and Zhu (2005) on terra rossa from the Guizhou province (China). They observed a very weak magnetic fabric in the terra rossa that was distinct from that in typical eolian deposits, and they suggested that the formation of terra rossa was a "special sedimentary process." Calculations by Brimhall and Dietrich (1987 and later papers) based on an assumed local conservation of one or another supposedly immobile element yielded gains or losses of bulk volume during saprolitization. These predicted volume changes are in conflict with (1) the paleomagnetic findings reported in this article for terra rossa and those reported by

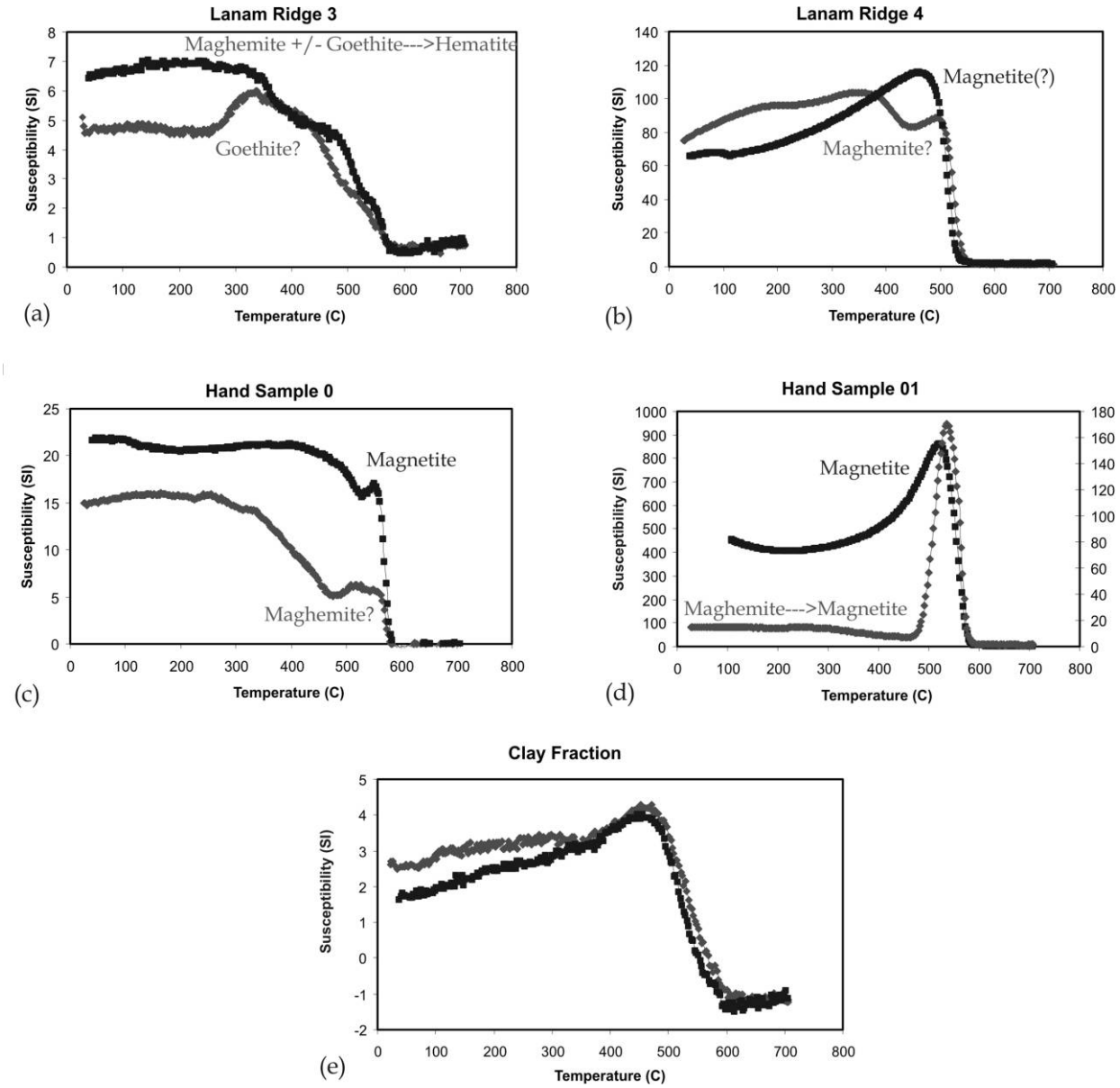

Figure 9. Curie temperature results (*light gray* = heating curve, *dark gray* = cooling curve) from sample LAN-3 showing a conversion of maghemite and/or goethite to hematite on heating (*a*), sample LAN-4 showing a mostly reversible Curie temperature curve of maghemite (*b*), Curie temperature curve from sample HS-0 showing a conversion of maghemite o magnetite during heating (*c*), and Curie temperature curve for sample HS-1 showing a conversion of goethite to maghemite during heating followed by the conversion of maghemite to magnetite during cooling (*d*). *e*, Curie temperature curve for the clay-size fraction of terra rossa showing nearly reversible heating and cooling curves indicating no alteration of the magnetic mineralogy in the clay fraction.

Mathé et al. (1999) for two African laterites, (2) with many independent petrographic and field observations (such as, among many others, Millot et al. 1977, for calcretization of schists; Nahon 1986 for ferricretes; Nahon and Merino 1997 and references therein for lateritization in West Africa and Brazil; and Merino and Banerjee 2008, for the Bloomington terra rossa), and (3) with dynamic theory (Dewers and Ortoleva 1990; Nahon and Merino 1997, pt. 2). These discoveries (1–3) point to isovolumetric saprolitization and terra rossa formation.

Note Added in Proof

In our revised manuscript, we overlooked citing the following article: Mathé, P. E.; Rochette, P.;

and Colin, F. 1997. The origina of magnetic susceptibility and its anisotropy in some weathered profiles. Physics and Chemistry of the Earth 22: 183–187.

ACKNOWLEDGMENTS

Thanks to C. Pullen, E. Tamrat, and J. Spearman for help in collecting samples; L. Gregory for comments on a draft; J. R. Dodd of Indiana University for help in the characterization of the Salem and Harrodsburg Limestones; and J.-L. Feng of the Institute of Tibetan Plateau Research of the Chinese Academy of Sciences for pointing out his 2003 and 2005 articles to us. Thanks also to D. Elmore and J. Geissman for very detailed comments that vastly improved the manuscript.

REFERENCES CITED

Brimhall, G. H., and Dietrich, W. E. 1987. Constitutive mass balance relations between chemical composition, volume, density, porosity and strain in metasomatic hydrochemical systems: results on weathering and pedogenesis. Geochim. Cosmochim. Acta 51: 567–587.

Dewers, T., and Ortoleva, P. 1990. Force of crystallization during growth of siliceous concretions. Geology 18: 204–207.

Feng, J.-L.; Cui, Z.-j.; Zhang, W.; Liu, G.-n.; and Zhu, L. 2003. Paleomagnetic dating of terra rossa profiles from Yun-Gui platform, SW China. Carsologica Sinica 22: 178–190 (in Chinese).

Feng, J.-L., and Zhu, L. 2005. Features and genetic implication of the magnetic fabric of terra rossa on dolomite. Carsologica Sinica 24:270–275 (in Chinese).

Fisher, R. A. 1953. Dispersion on a sphere. Proc. R. Soc. A 217:295–305.

Hanesch, M.; Stanjek, H.; and Petersen, N. 2006. Thermomagnetic measurements of soil iron minerals: the role of organic carbon. Geophys. J. Int. 165:53–61.

Heller, F. 1978. Rock magnetic studies of Upper Jurassic limestones from southern Germany. J. Geophys. 44: 525–543.

Mathé, P. E.; Rochette, P.; Vandamme, D.; and Colin, F. 1999. Volumetric changes in weathered profiles; isoelement mass balance method questioned by magnetic fabric. Earth Planet. Sci. Lett. 167:255–267.

McElhinny, M. W., and McFadden, P. L. 2000. Paleomagnetism: continents and oceans. International Geophysics Series. Vol. 73. San Diego, CA, Academic Press, 386 p.

Merino, E., and Banerjee, A. 2008. Terra rossa genesis, implications for karst, and eolian dust: a geodynamic thread. J. Geol. 116:62–75.

Merino, E., Nahon, D., and Wang, Yifeng. 2008. Kinetics and mass transfer of pseudomorphic replacement: application to replacement of parent minerals and kaolinite by Al, Fe and Mn oxides during weathering. Am. J. Sci. 293:135–155.

Millot, G.; Nahon, D.; Paquet, H.; Ruellan, A.; and Tardy, Y. 1977 L'épigénie calcaire des roches silicatées dans les encroûtements carbonatés en pays subaride, Anti Atlas, Maroc. Sci. Géol. Bull. 30:129–152.

Nahon, D. 1986. Evolution of iron crusts in tropical landscapes. *In* Colman, S. H., and Dethier, D. P., eds. Rates of chemical weathering of rocks and minerals. San Diego, CA, Academic Press, p. 169–191.

Nahon, D., and Merino, E. 1997. Pseudomorphic replacement in tropical weathering: evidence, geochemical consequences, and kinetic-rheological origin. Am. J. Sci. 297:393–417.

Opdyke, N. D., and Channell, J. E. T. 1996. Magnetic stratigraphy. International Geophysics Series. Vol. 64. San Diego, CA, Academic Press, 346 p.

Pruett, F. D. 1959. A study of the magnetic properties of some residual soils. MA thesis, Indiana University, Bloomington, 58 p.